

# A numerical study of a confined turbulent wall jet with an external stream

Zhitao Yan<sup>1,2</sup>, Yongli Zhong<sup>\*2</sup>, Xu Cheng<sup>3</sup>, Rory P. McIntyre<sup>4</sup> and Eric Savory<sup>4</sup>

<sup>1</sup>School of Civil Engineering and Architecture, Chongqing University of Science & Technology, Chongqing 401331, China

<sup>2</sup>School of Civil Engineering, Chongqing University, Chongqing, China, 400045

<sup>3</sup>School of Civil Engineering, Southwest Jiaotong University, Chengdu 610031, China

<sup>4</sup>Department of Mechanical and Materials Engineering, the University of Western Ontario, London, Canada, N6A 5B9

(Received March 15, 2018, Revised June 27, 2018, Accepted July 8, 2018)

**Abstract.** Wall jet flow exists widely in engineering applications, including the simulation of thunderstorm downburst outflows, and has been investigated extensively by both experimental and numerical methods. Most previous studies focused on the scaling laws and self-similarity, while the effect of lip thickness and external stream height on mean velocity has not been examined in detail. The present work is a numerical study, using steady Reynolds-Averaged Navier Stokes (RANS) simulations at a Reynolds number of  $3.5 \times 10^4$ , of a turbulent plane wall jet with an external stream to investigate the influence of the wall jet domain on downstream development of the flow. The comparisons of flow characteristics simulated by the Reynolds stress turbulence model closure (Stress-omega, SWRSM) and experimental results indicate that this model may be considered reasonable for simulating the wall jet. The confined wall jet is further analyzed in a parametric study, with the results compared to the experimental data. The results indicate that the height and the width of the wind tunnel and the lip thickness of the jet nozzle have a great effect on the wall jet development. The top plate of the tunnel does not confine the development of the wall jet within  $200b$  of the nozzle when the height of the tunnel is more than  $40b$  ( $b$  is the height of jet nozzle). The features of the centerline flow in the mid plane of the 3D numerical model are close to those of the 2D simulated plane wall jet when the width of the tunnel is more than  $20b$ .

**Keywords:** wall jet; confined; computational fluid dynamics; numerical simulation; Reynolds stress models

## 1. Introduction

A downburst is a strong downdraft inducing a damaging wind on or near the ground and attracting much attention in the meteorological and wind engineering fields (Fujita 1985, Chay and Letchford 2002, Lin and Savory 2010, Huang *et al.* 2015, Huang *et al.* 2016, Sim *et al.* 2016, Damatty and Huang 2018). The vertical profiles of the radial outflow velocity of a downburst, which reaches a peak magnitude and then decreases gradually, differs from that in the atmospheric boundary layer (e.g., Wood *et al.* 2001, Peng *et al.* 2018). The conventional way of achieving downburst outflow similarity is the impinging jet approach (Chay and Letchford 2002, Letchford and Chay 2002, Tang and Lu 2013). Because the impingement regime is smaller than the outflow wall jet regime, the probability of damage to a structure in the impingement regime is also smaller. In addition, the horizontal winds in the wall jet regime tend to be very disruptive to high-rise structures. The increased pressure beneath a downburst mainly exists in the impingement regime and is less hazardous for such structures. Lin and Savory (2006, 2010) sought a better solution to this practical engineering simulation problem by generating a large-scale outflow that is very similar to that of a downburst. They showed that a plane wall jet arising from a rectangular slot nozzle can adequately represented a

downburst outflow.

A turbulent wall jet is a shear flow directed along a wall, where, by virtue of the initially supplied momentum, at any downstream station, the streamwise velocity over some region within the flow exceeds that in the external stream (Launder and Rodi 1981). Wall jet is generally considered to be composed of two layers. The inner layer is similar to the turbulent boundary layer while the outer layer behaves like a free shear layer. These two layers interact with each other strongly so that wall jets form a complex flow field. In addition to downbursts, wall jet flows are common in engineering applications, such as film cooling in gas turbines and boundary-layer control by blowing (Pajayakrit 1997). There also exists an external flow in most practical situations. In the case of downburst outflow simulation by a wall jet an external stream may be applied to simulate a translating event (Lin and Savory 2006, 2010). Thus, it is of important significance for engineering practice to clarify the behavior of the wall jet and to accurately predict its features.

The characteristics of a turbulent plane wall jet without an external stream have been studied in detail. Launder and Rodi (1981) reviewed the experimental literature up to 1980. After that, more experimental studies were carried out (Wynanski *et al.* 1992, Abrahamsson *et al.* 1994, Eriksson *et al.* 1998, Rostamy *et al.* 2009). Bradshaw and Gee (1960) made early experimental studies on wall jets with an external stream. They found that the jet absorbed the boundary layer within a short distance when the ratio of initial jet momentum thickness to initial boundary-layer momentum deficit thickness was less than 5. A variety of

\*Corresponding author, Ph.D.  
E-mail: zhongyongli@cqu.edu.cn

experiments of wall jet with an external stream were further conducted by Zhou and Wygnanski (1993) who examined the influence of the initial velocity ratio and Reynolds number on the development of the wall jet. Their experiments used ratios from 0.085 to 0.93 and they found that the rate of spread was greatly affected by the velocity ratio. However, neither the velocity ratio nor Reynolds number had a significant effect on the maximum velocity height.

Another important factor impacting the wall jet with an external stream is the geometry of the wall jet domain. Kacker and Whitelaw (1971) carried out comprehensive experiments for four values of the velocity ratio with two lip thickness. The values of the ratio of lip thickness to slot height were 0.126 and 1.14. They showed that the lip thickness had an influence on the velocity profile and turbulence quantities close to the jet nozzle. In the simulation of a downburst outflow using the plane wall jet method, the effect of nozzle lip thickness cannot be ignored. It is also a key parameter to which film effectiveness is correlated in film-cooling and so it is necessary to study the effect of nozzle lip thickness. A wall jet entrains fluid from the surroundings and in numerical simulations this entraining fluid has to be provided through boundary conditions. There are various ways to do this. One can define small co-flow (Ahlman *et al.* 2007, Naqavi *et al.* 2017), the vertical velocity at the top-wall can be defined (Dejoan and Leschziner 2005, Banyassady and Piomelli 2015) or a “no inflow” condition can be defined which generates a recirculation region above the wall jet and results in a reduction of the effective domain length (Levin *et al.* 2006). If no co-flow or vertical velocity is defined, then the effective domain length can be limited by the height of the domain (Swean *et al.* 1989). It is necessary to study the effect of external stream height to determine whether the wall jet is fully developed and is confined by the top plate of wind tunnel. In order to clarify the effect of varied co-flow height and varied plate thickness on the wall jet, a series of tests were carried out by McIntyre (2011). He found that the lip thickness affected the maximum velocity, but no obvious regularity was observed, and the different tunnel heights examined identified that the role of the upper boundary far downstream was to reduce the two-dimensionality of the flow and remove the upper portion of the wall jet velocity profile from the flow.

Study of the turbulent wall jet has also progressed by numerical simulation with Computational Fluid Dynamics (CFD). Tangemann and Gretler (2001) simulated a wall jet with an external stream for three velocity ratios. A combined algebraic stress model with a two-equation turbulence model was proposed to improve predictions of the negative production of turbulent kinetic energy. By large eddy simulation (LES), Naqavi *et al.* (2014) studied the interaction of the wall jet with an external stream for velocity ratios in the range 0.3-2.3. Ayeche *et al.* (2016) used a modified Low-Reynolds number  $k-\varepsilon$  model to investigate an isothermal and a non-isothermal turbulent plane wall jet emerging in a co-flow stream with different velocity ratios ranging from 0 to 0.2. They found that the effect of the velocity ratio is negligible close to the nozzle exit and that

the spread rate of the wall jet increases for lower velocity ratios while the maximum velocity decreases.

The previous numerical simulations of a wall jet with an external stream mainly focused only on the velocity ratio, while the geometry of wall jet domain has not been investigated in detail. A better understanding of the effect of nozzle lip thickness and external stream height is very significant for engineering applications. Yan *et al.* (2018) used seven RANS turbulence models to simulate the 2-D plane wall jet without co-flow. They found that the stress-omega Reynolds stress model (SWRSM) with adjusted turbulence model constants gave the best results for simulating a steady wall jet without co-flow. In the current study, the Reynolds stress model (RSM) with Stress-Omega model (SWRSM) has been used to simulate the experiment of McIntyre (2011), which is a confined wall jet, and variations of the geometric parameters are taken into account. The numerical results are compared with the experimental data in the literature. Then, the results of the wind tunnel parametric analysis are presented and discussed.

## 2 Problem formulation

### 2.1 Governing equations

The conservation equations of mass and momentum for incompressible fluid flow can be expressed as follows

$$\frac{\partial u_i}{\partial x_i} = 0 \quad (1)$$

$$\frac{\partial}{\partial x_j} (\rho u_i u_j) = -\frac{\partial p}{\partial x_i} + \frac{\partial \tau_{ij}}{\partial x_j} + \frac{\partial}{\partial x_j} (\mu \frac{\partial u_i}{\partial x_j}) \quad (2)$$

where  $\rho$  is the fluid density;  $u_i$ ,  $u_j$  are the velocity components corresponding to  $i$  and  $j$ , respectively,  $p$  is the pressure,  $\mu$  is the fluid dynamic viscosity,  $\tau_{ij} = -\overline{\rho u_i u_j}$  are the Reynolds stresses.

The turbulence model adopted for the turbulence closure problem is a revised version of the Stress-omega turbulence model. This model was proposed by Wilcox (1998) and modified by Wilcox (2006). The modified constants improved the performance of the turbulence model. In this study, the model constants used in the RSM (Stress-omega) are as Table 1.

### 2.2 Flow configuration

The 3D models with the SWRSM turbulence model have been used to simulate the experiment, which is a confined wall jet and variations of geometric parameters are taken into account. A representative simulation domain was configured based on the experimental setup in McIntyre (2011). As shown in Fig. 1, where the slot nozzle height  $b = 12.7$  mm, and the width  $w = 360$  mm. The jet flow is a confined wall jet with a weak co-flow ( $U_E/U_j \approx 10\%$ ).

Table 1 Model constants of SWRSM

$C_1$	$C_2$	$\text{Alpha}^*_\text{inf}$	$\text{Alpha}_\text{inf}$	$\text{Beta}_\text{i}$	$\text{Beta}^*_\text{inf}$	$\text{zeta}^*$	$\text{Mt0}$	TKE Prandtl number	SDR Prandtl number
1.8	10/19	1	0.52	0.0708	0.09	0.5	0.25	5/3	2

Table 2 The cases of simulation and experiment

Cases	Simulation		Cases	Experiment	
	$t$	$h$		$t$	$h$
S1	0.125b	5b			
S2	0.125b	10b	E1	0.125b	10b
S3	0.125b	13b	E2	0.125b	13b
S4	0.125b	16b	E3	0.125b	16b
S5	0.125b	20b	E4	0.125b	20b
S6	0.125b	40b			
S7	0.125b	60b			
S8	0.125b	60b-no top plate			
S9	0.05b	20b			
S10	0.5b	20b	E5	0.5b	20b
S11	1b	20b	E6	1b	20b
S12	2b	20b	E7	2b	20b

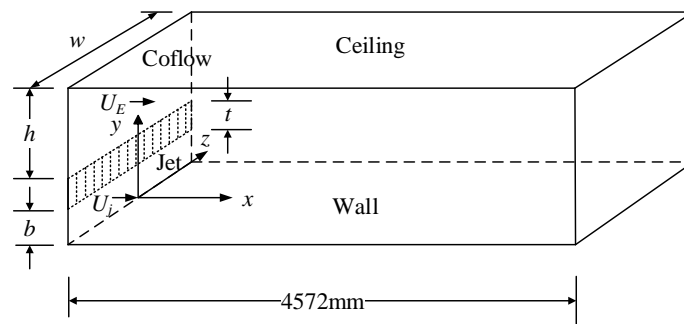


Fig. 1 Working section details in the experiment, McIntyre (2011)

The measurement plane is located in the center of the domain ( $y=0$ ), and aligned with the  $x$  axis. The downstream distances from the jet inlet where measurements were taken are  $10b$ ,  $20b$ ,  $40b$ ,  $60b$ ,  $80b$ ,  $100b$ ,  $120b$ ,  $140b$ ,  $180b$ ,  $200b$ , respectively. The instantaneous velocities of every point were measured by crossed hot-wire anemometry, from which the mean velocities and Reynolds stresses were obtained. Two geometric lengths varied in the experiment, the co-flow height ( $h$ ) and the lip thickness ( $t$ ), while the width  $w$  is another geometrical length that was varied only in the numerical simulations. The cases of simulation and experiment are shown in Table 2.

### 2.3 Boundary conditions

For comparison with possible future computational studies, the experimental study of McIntyre (2011) provided well defined conditions. Hence, the mean profiles of the wall jet and co-flow at the inlet are available from the experiment and were used as the inlet conditions in the numerical simulations. The Reynolds number of the jet was  $3.5 \times 10^4$  based on the nozzle height and the nozzle exit jet velocity of 40 m/s. Fig. 2 shows the inflow condition of the typical case of S5. The uniform co-flow provides the fluid

for the jet entrainment. The top, bottom and lateral walls are set as no-slip boundaries. The outflow is specified as a convective boundary condition (Orlanski 1976).

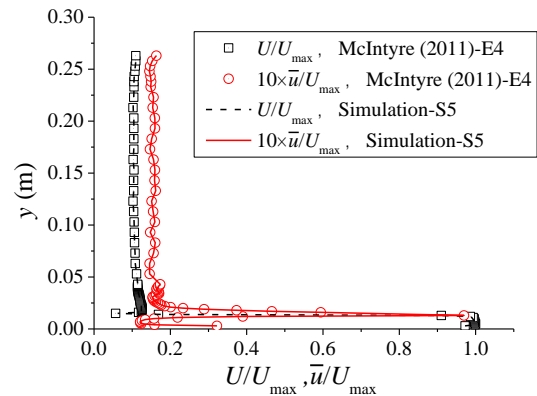


Fig. 2 Inlet velocity and turbulence intensity profiles of the simulation and experiment

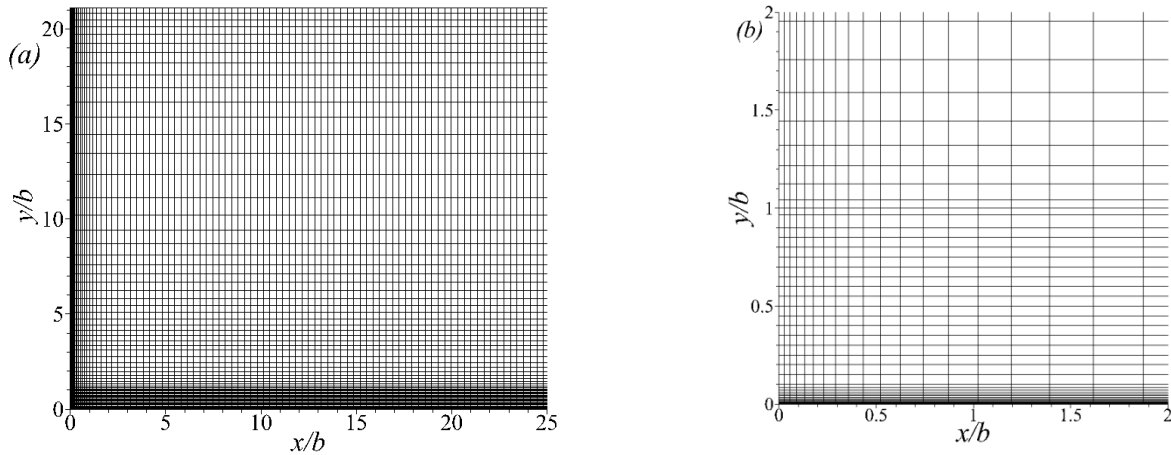


Fig. 3 (a) Computational mesh in the  $x$ - $y$  plane in the region  $x/b < 25$  and (b) close-up view in the vicinity of the nozzle exit ( $x/b < 2$ ,  $y/b < 2$ )

### 2.4 Solution approach

All numerical simulations are performed in the framework of the commercial flow solver ANSYS Fluent 17.0. The continuity and momentum equations were solved simultaneously and a spatial second-order upwind scheme was employed for momentum, specific dissipation rate and the Reynolds stresses equations. The spatial gradient is discretized with Least Squares Cell Based Method and the pressure discretization method is Standard.

The SIMPLEC scheme is chosen to provide a better convergence (lower convergence residuals) compared with the pressure-implicit with the splitting of operators (PISO) scheme. The absolute convergence criteria of continuity, velocities in the  $x$  and  $y$  directions,  $\omega$ ,  $\varepsilon$ , kinetic energy and Reynolds stress were  $1 \times 10^{-6}$ .

### 3. Validation of numerical results

All grids were structured grids with the wall region strenuously refined. For a typical case S5 (see Table 1), the total number of elements is 1,336,720 (Grid 1), and the node number is 1,453,040. The nearest grid point to the bottom wall is located at  $\Delta y^+$  of less than 2. In the streamwise and spanwise direction, the resolution of the wall units is  $\Delta x^+ < 126$  and  $\Delta z^+ < 93$  respectively. Grid dependency tests were performed with a finer grid (Grid 2, element number is 2,673,440). The resolution of this grid, in local units, is  $\Delta x^+ < 88$ ,  $\Delta y^+ < 1$  and  $\Delta z^+ < 96$ . The grid numbers of the other cases are proportionally increased with geometric size to keep the same element size. Fig. 3 shows the computational mesh in the  $xy$ -plane in the region  $x/b < 25$  and a close-up of the computational mesh in the vicinity of the jet exit for the typical case S5.

The mean streamwise velocity and Reynolds shear stress profiles of typical case S5 at the location of  $x=20b$  are shown in Figs. 4 and 5, respectively. The results obtained from the two grids are in very good agreement and no

noticeable variance in the mean velocity profiles was observed. The maximum difference in the Reynolds shear stress profiles between two grids is found to be less than 3%. The grid effects are almost insignificant and this indicates the independency of the results on the grids. Only Grid 1 is employed for the simulations presented here.

The typical cases of S5 and E4 are analyzed as follows and similar conclusions can be obtained from the other comparisons. The mean velocity profiles obtained with the SWRSM model match the McIntyre's experiments (2011) very well. All the mean velocity profiles normalized by  $U_m$  in different cross sections can be collapsed onto a universal curve by using the half-width,  $y_{1/2}$ , to scale the profile vertical locations (where the half-width corresponds to the location where  $U/U_m = 0.5$ ). Fig. 6 shows good agreement between the typical experimental and numerical result at  $x=100b$ . The velocity profiles from wall jets also match well an empirical model of a downburst (Wood *et al.* 2001).

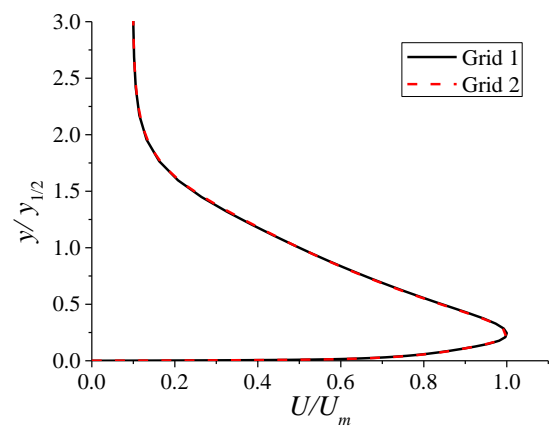


Fig. 4 The mean velocity profiles at  $x=20b$  with two different grids

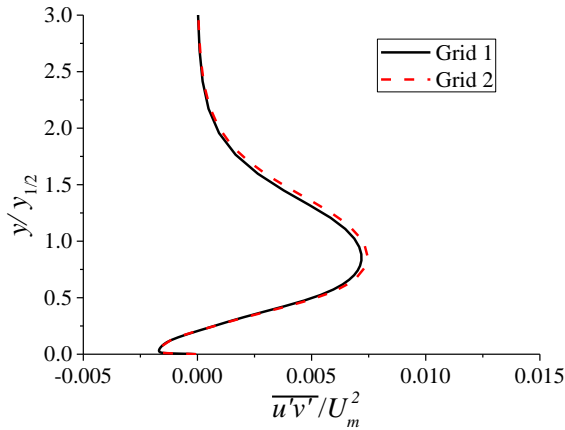


Fig. 5 The mean Reynolds shear stress profiles at  $x=20b$  with two different grids

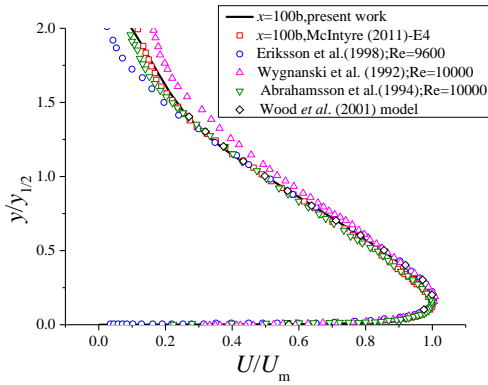


Fig. 6 The normalized mean velocities of the CFD simulation and the experiment ( $x=100b$ )

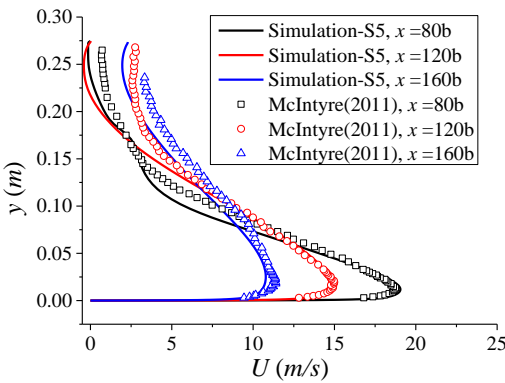


Fig. 7 The non-normalized mean velocities of the CFD simulation and the experiment

Almost all investigators use the maximum velocity,  $U_m$ , to normalize the velocity in order to obtain similarity of profiles. However, it is not possible to truly judge the fidelity of the comparison of experiment and simulation

solely by these normalized velocity profiles (Klinzing and Sparrow 2009). In order to achieve a more quantitative comparison between the experiment and simulation, the velocity and y-coordinate are used directly. As shown in Fig. 7, the velocity profiles from the numerical predictions match well with experimental data at different streamwise locations.

The Reynolds stresses of the simulations and experiments cannot be collapsed onto one curve normalized by  $U_m^2$  and  $y_{1/2}$  in the confined wall jet, encompassing a range of downstream locations. Hence, here the comparisons are made at a single cross section of  $x=100b$ ,

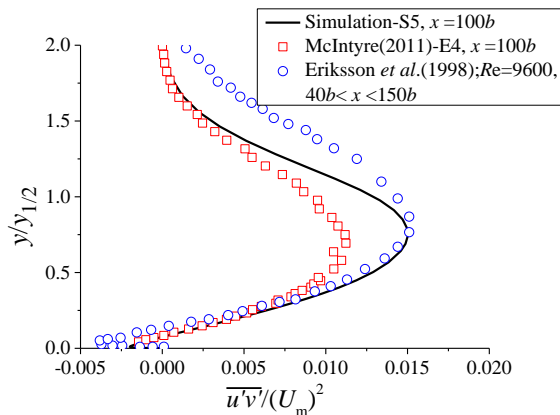
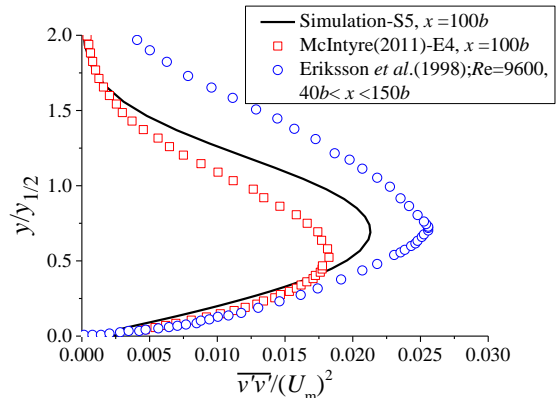
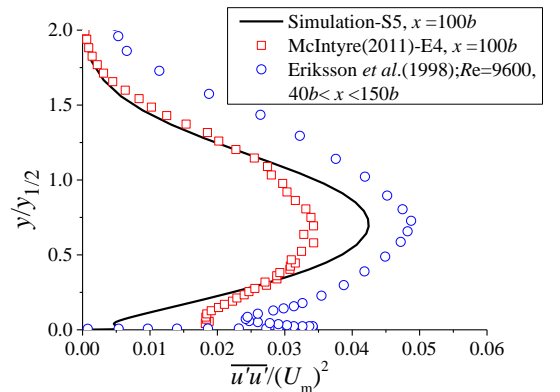


Fig. 8 The Reynolds Stresses of the CFD simulation and the experiment ( $x=100b$ )

as shown in Fig. 8. The Reynolds stresses of the simulation (S5) are about 20% larger than those of the wind tunnel tests (E4), which is reasonable because the experimental stresses were measured by hot-wire anemometry which usually records larger magnitudes of Reynolds stress compared to those measured by LDV, according to Eriksson *et al.* (1998). Furthermore, the inner peak of the streamwise normal stress of the prediction is not obvious and far smaller in magnitude than the results of the experimental studies of McIntyre (2011) and Eriksson *et al.* (1998). However, since the focus of this study is the downstream development of the velocity profiles, use of the Reynolds stress model (RSM) with the Stress-Omega model (SWRSM) may be considered reasonable.

#### 4. Wind tunnel parameter analysis

##### 4.1 Variation of co-flow height

All the scaling, such as half-height, the decay of maximum velocity, the relation of  $U_m$  and  $y_{1/2}$  *etc.* of the numerical simulation with the SWRSM turbulence model also match very well with the experimental data of the confined wall jet. The comparisons between the half-heights of the simulations and those of the experiments are shown in Fig. 9. Because of the confining effect of the top tunnel plate, the half-height variation is not linear with downstream distance after 100*b*.

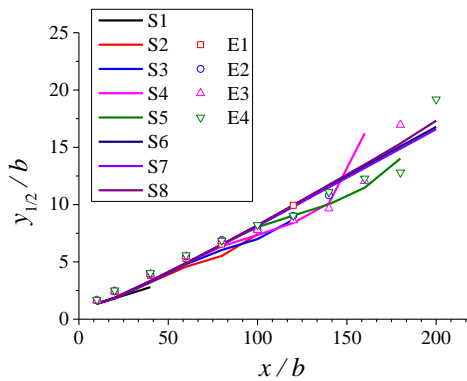


Fig. 9 Half-height  $y_{1/2}/b$  versus  $x/b$

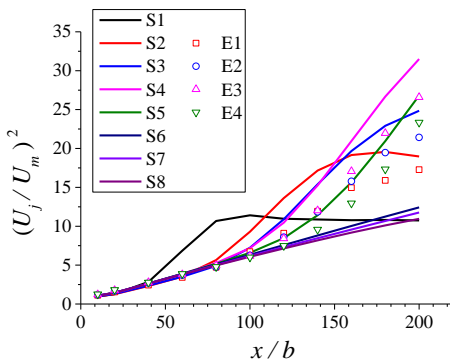


Fig. 10  $(U_j/U_m)^2$  versus  $x/b$

The additional cases analyzed by CFD indicate that the linear segment of the half-height increases with increasing tunnel height because the top plate of the tunnel limits the development of the wall jet. The linear segment can reach  $200b$  when the tunnel height is larger than  $40b$ .

Fig. 10 shows that the scaling of the decay of maximum velocity varies with increasing tunnel height. The relation between  $(U_j/U_m)^2$  and  $x/b$  is linear when the height of tunnel is larger than  $40b$ . When the height is small, such as  $5b$ , and  $10b$ , the linear segment is short and there is an inflection in the curve. The maximum velocity decay is faster with increasing tunnel height.

The relation of  $U_m$  and  $y_{1/2}$  can also be normalized by and  $M_0$  where  $M_0$  is the rate at which momentum per unit mass and unit length is added at the source. This jet scaling was shown to be independent of  $Re$  (Wyganski *et al.* 1992). The non-dimensional similarity can be written as Eq. (3), as was given by George *et al.* (2000).

$$\frac{U_m v}{M_0} = B_1 \left( y_{1/2} M_0 / v^2 \right)^n \quad (3)$$

where  $B_1$  and  $n$  are constants determined by fitting experimental data and equal to 1.85 and -0.528, respectively. Fig. 11 shows that the relations  $U_m v/M_0$  and  $y_{1/2} M_0 / v^2$  accord with George's theory very well when the height of the tunnel is larger than  $40b$ . The linear segment becomes shorter when the tunnel height is lower.

Fig. 12 shows the contours of mean streamwise velocity for different tunnel height in central plane. It is seen that the restriction of the upper boundary on the wall jet is very obvious when the tunnel heights are  $5b$  and  $10b$ . The development of the wall jet is not affected up to the streamwise position  $x/b=80$  for  $h/b=20$ . When the tunnel height is  $40b$ , wall jets are hardly confined by the top plate of the tunnel and this is consistent with the above analysis.

##### 4.2 Variation of tunnel width

Several cases with different widths, such as  $w = 10b$ ,  $15b$ ,  $20b$ ,  $25b$  and  $30b$  and the same tunnel width as in the experiment ( $w = 28.34b$ ) were simulated with the SWRSM model.

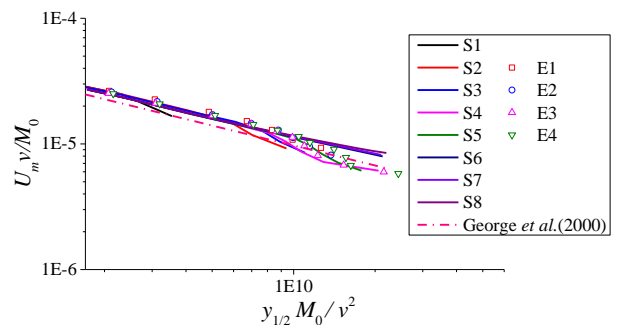


Fig. 11 The momentum similarities about the maximum velocity and the half-height

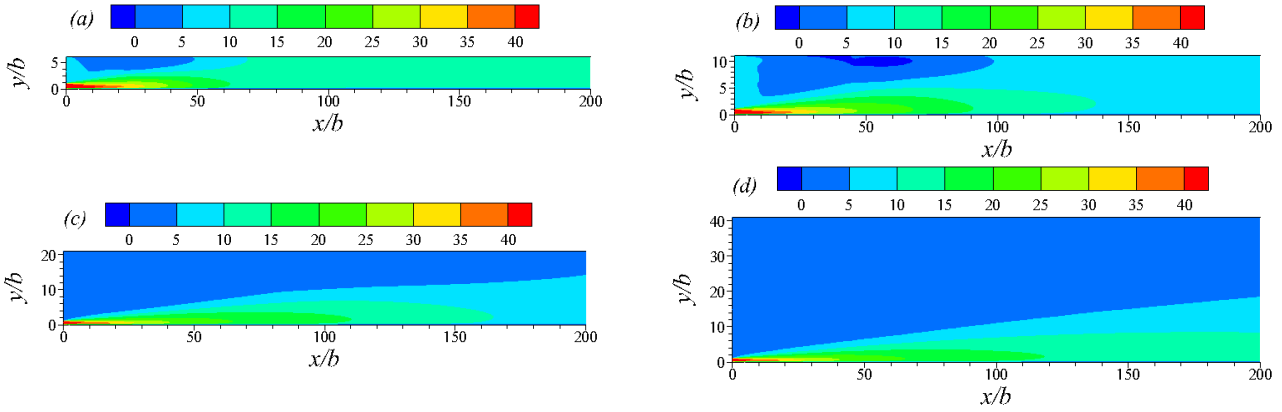


Fig. 12 Contours of mean velocity magnitude for the confined wall jet with co-flow. (a)  $h/b=5$ , (b)  $h/b=10$ , (c)  $h/b=20$  and (d)  $h/b=40$ . (CFD data)

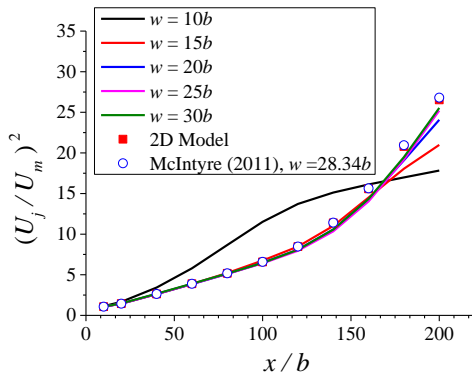


Fig. 13 The  $(U_j/U_m)^2$  versus  $x/b$  for different tunnel widths

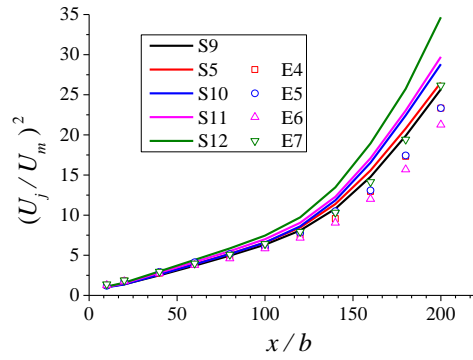


Fig. 15 The  $(U_j/U_m)^2$  versus  $x/b$  for different plate thicknesses

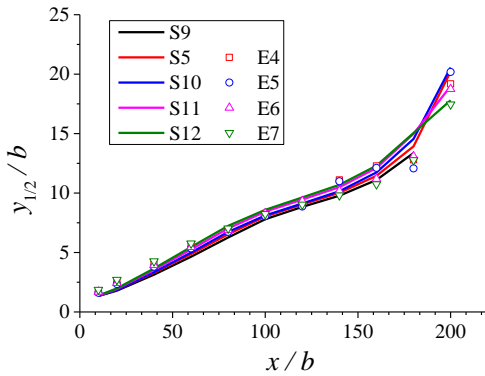


Fig. 14 Half-height  $y_{1/2}/b$  versus  $x/b$

The results of the simulations show that the wall jet will lose its two dimensionality when the width is less than  $15b$ .  $(U_j/U_m)^2$  of the simulations match that of the experiment very well when the tunnel width is larger than  $20b$ . When the width increases to  $30b$ ,  $(U_j/U_m)^2$  of the 3D model is close to that of the 2D CFD model, as shown in Fig. 13.

### 4.3 Variation of lip thickness of jet nozzle

The simulations of the confined wall jet with different jet nozzle lip thicknesses show no apparent influence on the half-height  $y_{1/2}/b$  for  $h=20b$ , as shown in Fig. 14. However,  $(U_j/U_m)^2$  increases with increasing plate thickness  $t$ , as shown in Fig. 15. The discrepancies between case S9 and case S12 will be up to 40% when  $x/b = 200$ .

## 5. Conclusions

In the present study, the steady, turbulent confined wall jet was simulated numerically using the Reynolds-Averaged Navier-Stokes (RANS) equations with the Reynolds stress turbulence closure incorporating the Stress-Omega model at a Reynolds number of  $3.5 \times 10^4$ , based on the slot nozzle height ( $b = 13 \text{ mm}$ ) and the jet exit velocity  $U_j = 40 \text{ m/s}$ . The simulations covered the mean velocity profile, Reynolds stresses, rate of spread and the decay of maximum velocity for various tunnel geometries. The numerical results were then compared with previous experimental measurements.

The simulation results showed that Reynolds stress model with Stress-Omega model from Wilcox (2006) provided a good prediction for the mean velocity profiles of wall jet with an external stream. Compared with the experiment of McIntyre (2011), both normalized and non-normalized profiles of velocity could be predicted well, while the ability to predict the turbulence characteristics was relatively poor, which could be attributed to the weakness of the wall functions used in the simulations.

The parametric study of the confined plane wall jets demonstrated that the height and the width of the tunnel and the jet nozzle lip thickness had a great impact on the development of the wall jet. When the height was about  $40b$  ( $b$  is the height of jet), the top plate of the tunnel would not confine the development of the wall jet up to a downstream distance of  $200b$ . When the width was more than  $20b$ , the flow features at the center plane of the 3D model were similar to those of the 2D simulated plane wall jet. When the confined wall jet method was used to simulate a downburst outflow, the height of the tunnel should be greater than  $40b$ . At the same time, the width of the tunnel should be larger than  $20b$  in order to maintain the two-dimensionality of the wall jet.

## Acknowledgements

This work was supported by National Natural Science Funding (China, 51478069, 51778097) and Chongqing Natural Science Funding (cstc2017jcyjB0210).

## References

- Abrahamsson, H., Johansson, B. and Löfdahl, L. (1997), "A turbulent plane two-dimensional wall-jet in a quiescent surrounding", *Eur. J. Mech. s / B-Fluid.*, **13**(5), 533-556.
- Ahlman D., Brethouwer, G. and Johansson, A.V. (2007), "Direct numerical simulation of a plane turbulent wall-jet including scalar mixing", *Phys. Fluid.*, **19**, 065102.
- Ayech, S.B.H., Habli, S., Saïd, N.M., Bournot, P. and Palec, G.L. (2016), "A numerical study of a plane turbulent wall jet in a coflow stream", *J. Hydro-Environ. Res.*, **12**, 16-30.
- Banyassady, R. and Piomelli, U. (2015), "Interaction of inner and outer layers in plane and radial wall jets", *J. Turbul.*, **16**(5), 460-483.
- Bradshaw, B. and Gee, M. (1962), "Turbulent wall jets with and without an external stream", *Aeronautical Research Council Report and Memoranda*, No. 3252, HM Stationery Office, U.K.
- Chay, M.T. and Letchford, C.W. (2002), "Pressure distributions on a cube in a simulated thunderstorm downburst. part B: moving downburst observations", *J. Wind Eng. Ind. Aerod.*, **90**(7), 733-753.
- Dejoan, A. and Leschziner, M.A. (2005), "Large eddy simulation of a plane turbulent wall jet", *Phys. Fluid.*, **17**, 025102.
- El Damatty, A. and Huang, G. (2018), "Special issue on Non-Synoptic Wind I Preface", *Wind Struct.*, **26**(3).
- Eriksson, J.G., Karlsson, R.I. and Persson, J. (1998), "An experimental study of a two-dimensional plane turbulent wall jet", *Exp. Fluids*, **25**(1), 50-60.
- Fujita, T.T. (1985), The downburst : microburst and macroburst : report of projects NIMROD and JAWS. Satellite and Mesometeorology Research Project, Dept. of the Geophysical Sciences, University of Chicago.
- George, W.K., Abrahamsson, H. and Löfdahl, L. (1996), "A similarity theory for the plane wall jet", *Eng. Turbul. Model. Exp.*, 677-686.
- Huang, G., Zheng, H., Xu, Y.L. and Li, Y. (2015), "Spectrum models for nonstationary extreme winds", *J. Struct. Eng.*, **141**(10), 04015010.
- Huang, G., Su, Y., Kareem, A. and Liao, H. (2015), "Time-frequency analysis of nonstationary process based on multivariate empirical mode decomposition", *J. Eng. Mech.*, **142**(1), 04015065.
- Kacker, S.C. and Whitelaw, J.H. (1971). "The turbulence characteristics of two dimensional wall-jet and wall-wake flows", *J. Appl. Mech.*, **38**(1), 239-251.
- Klinzing, W. and Sparrow, E. (2009), "Evaluation of turbulence models for external flows", *Numer. Heat Transfer*, **55**(3), 205-228.
- Launder, B.E. and Rodi, W. (1981), "The turbulent wall jet", *Prog. Aerosp. Sci.*, **19**(79), 81-128.
- Letchford, C.W. and Chay, M.T. (2002), "Pressure distributions on a cube in a simulated thunderstorm downburst-Part A: stationary downburst observations", *J. Wind Eng. Ind. Aerod.*, **90**(7), 711-732.
- Levin, O., Herbst, A.H. and Henningson, D.S. (2009), "Early turbulent evolution of the Blasius wall jet", *J. Turbul.*, **7**, (68).
- Lin, W.E. and Savory, E. (2006), "Large-scale quasi-steady modelling of a downburst outflow using a slot jet", *Wind Struct.*, **9**(6), 419-440.
- Lin, W.E. and Savory, E. (2010), "Physical modelling of a downdraft outflow with a slot jet", *Wind Struct.*, **13**(13), 385-412.
- McIntyre R.P. (2011), "The effect of inlet geometry on the development of a plane wall jet", M.E.Sc. thesis, University of Western Ontario, London, Canada.
- Naqavi, I.Z., Paul G.T. and Liu, Y. (2014), "Large-eddy simulation of the interaction of wall jets with external stream", *Int. J. Heat Fluid Fl.*, **50**, 431-444.
- Naqavi, I.Z., James C.T. and Paul G.T. (2016), "A numerical study of a plane wall jet with heat transfer", *Int. J. Heat Fluid Fl.*, **63**, 99-107.
- Orlanski, I. (1976), "A simple boundary condition for unbounded hyperbolic flows", *J. Comput. Phys.*, **21**(3), 251-269.
- Pajayakrit, P. (1997), Turbulence modeling for curved wall jets under adverse pressure gradient, Ph.D. thesis, Carleton University, Ottawa, Canada.
- Peng, L., Huang, G., Chen, X. and Yang, Q. (2018), "Evolutionary spectra-based time-varying coherence function and application in structural response analysis to downburst winds", *J. Struct. Eng.*, **10.1061/(ASCE)ST.1943-541X.0002066**.
- Rostamy, N., Bergstrom, D.J., Deutscher, D., Sumner, D. and Bugg, J.D. (2009), "An experimental study of a plane turbulent wall jet using LDA, Paper 670, Turbulence", Heat and Mass Transfer 6, Proc. 6<sup>th</sup> Int. Symp. Turb., Heat and Mass Trans., Rome, Italy, September, Begel House Inc.
- Sim, T.S., Ong, M.C., Quek, W.Y., Zheng, W.S., Lai, W.X. and Skote, M. (2016). "A numerical study of microburst-like wind load acting on different block array configurations using an impinging jet model", *J. Fluid. Struct.*, **61**, 184-204.
- Swean, T.F., Ramberg, S.E., Plesniak, M.W. and Stewart, M.B. (1989). "Turbulent surface jet in channel of limited depth", *J. Hydraul. Eng. -ASCE*, **115**(12), 1587-1606.
- Tang, Z. and Lu, L. (2013), "A proposed model of the pressure field in a downburst", *Wind Struct.*, **17**(2), 123-133.
- Tangemann, R. and Gretler, W. (2000), "Numerical simulation of a two-dimensional turbulent wall jet in an external stream", *Forschung Im Ingenieurwesen*, **66**(1), 31-39.
- Wilcox, D.C. (1998), Turbulence modeling for CFD (Second

- Edition). DCW Industries La Canada California USA.
- Wilcox, D.C. (2006), *Turbulence Modeling for CFD* (Third Edition). DCW Industries La Canada California USA.
- Wood, G.S., Kwok, K.C.S., Motteram, N.A. and Fletcher, D.F. (2001), "Physical and numerical modelling of thunderstorm downbursts", *J. Wind Eng. Ind. Aerod.*, **89**(6), 535-552.
- Wynanski, I., Katz, Y. and Horev, E. (1992), "On the applicability of various scaling laws to the turbulent wall jet", *J. Fluid Mech.*, **234**, 669-90.
- Yan, Z.T., Zhong, Y.L. and Lin, W.E. (2018), "Evaluation of RANS and LES turbulence models for simulating a steady 2-D plane wall jet", *Eng. Comput.*, **35** (1), 211-234.
- Zhou, M.D. and Wynanski, I. (2012), "Parameters governing the turbulent wall jet in an external stream", *AIAA J.*, **31**(31), 848-853.